

Unique Regioselective Binding of Permethylated β -Cyclodextrin with Azobenzene Derivatives

Jun Shi,^[a] Dong-Sheng Guo,^[a] Fei Ding,^[a] and Yu Liu*^[a]

Keywords: Host–guest systems / Cyclodextrins / Inclusion compounds / Thermodynamics

The binding behavior of permethylated β -cyclodextrin (PM- β -CD) upon complexation with 4-hydroxyazobenzene (4-HAB) and 4-aminoazobenzene (4-AAB) was investigated by X-ray crystallography, circular dichroism, 2D NMR spectra, and isothermal titration calorimetry. In comparison to the reported β -cyclodextrin (β -CD) complexes with 4-HAB and 4-AAB, PM- β -CD complexes **3** and **4** present not only unique binding regioselectivity with azobenzene guests but also have distinct spatial arrangements, that is, β -CDs arrange in a head-to-head manner, whereas PM- β -CDs arrange in a

head-to-tail manner. The results obtained from circular dichroism and 2D NMR spectra indicate that the binding modes of complexes **3** and **4** in solution are in accordance with those in the solid state. Furthermore, the binding abilities and thermodynamic parameters of β -CD and PM- β -CD upon complexation with azobenzene derivatives were discussed from the viewpoints of the flexibilities of the frameworks of the hosts and driving forces.

(© Wiley-VCH Verlag GmbH & Co. KGaA, 69451 Weinheim, Germany, 2009)

Introduction

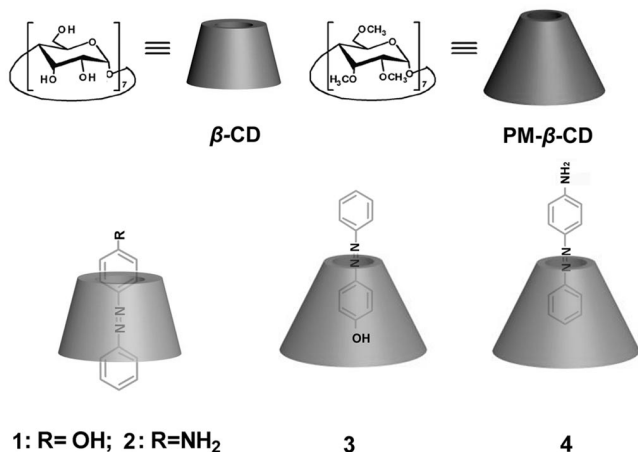
Supramolecular architectures constructed by cyclodextrin (CD) blocks, such as rotaxane,^[1–3] molecular shuttles,^[4] molecular tube,^[5] and so on prove to be of more interest in chemistry and materials science nowadays due to their fascinating properties including water solubility, biological consistency, and economics endowed by CD blocks upon their remarkable ability to include various guest molecules either in solution or in the solid state.^[6] A number of crystallographic studies on the CD-based inclusion complexes have been performed to obtain direct evidence for the formation of the inclusion complexes that can be subsequently used as building blocks to construct supramolecular aggregates.^[7,8] Moreover, among the CD derivatives, permethylated cyclodextrins (PMCDs), representing a new family of CD hosts, where all of the hydroxy groups of the CDs are methylated, are widely used as the solubilizing agent and as the hosts for encapsulating various organic molecules, including drugs, because of their patulous cavity,^[9] flexible framework,^[10] and better solubility in both aqueous and organic solution.^[7a,9] It is also interesting that PMCDs exhibit distinguishable inclusion complexation behaviors for some special substrates from CDs.^[11–13] For example, PM- β -CDs can afford binding constants up to 10^5 to 10^6 M⁻¹ with charged porphyrins in aqueous or aqueous/organic

media,^[12a] whereas β -CD only present around 10^3 M⁻¹ for complexation with porphyrins in aqueous solution.^[12c] However, the crystallographic investigations on the PMCD complexes are still not as mature as those of CD up to now.^[14] Harata and coworkers analyzed the crystal structures of PMCD complexes with some optically active guests such as mandelic acid^[14a] and flurbiprofen.^[14b] Petit and coworkers^[14c] obtained a pair of PM- β -CD complexes with racemic 1-(*p*-bromophenyl) by successive recrystallization and discussed the crystal structures and chiral discrimination mechanisms of PM- β -CD. Direct comparison of the complex structures between CD and PMCD with the same guests is especially reported less frequently,^[14d] which is significant to help us comprehend the differences of these two kinds of CD hosts, including binding geometries, driving forces of complexation, further aggregation topologies, and so on.

In a previous study, we reported two inclusion complexes of β -CD with 4-hydroxyazobenzene (4-HAB, **1**) and 4-aminoazobenzene (4-AAB, **2**), including their binding and assembly behavior both in aqueous solution and the solid state. The obtained results indicate that the positions of the substituents in the azobenzenes play an important role in inclusion complexation and molecular assembly.^[8d] Herein, we further obtained two inclusion complexes of PM- β -CD with 4-HAB (**3**) and 4-AAB (**4**) shown in Scheme 1, and their binding and assembly behaviors were studied by X-ray crystallography, circular dichroism, 2D NMR spectra, and isothermal titration calorimetry (ITC). To obtain deeper insight on the respective characteristics of CD and PMCD, their complexation structures and binding thermodynamics were systemically analyzed and discussed. More-

[a] Department of Chemistry, State Key Laboratory of Elemento-Organic Chemistry, Nankai University, Tianjin 300071, P. R. China
Fax: +86-22-2350-3625
E-mail: yuliu@nankai.edu.cn

over, it is also our interest to explore how the disparities of substituents of azobenzene guests affect the inclusion complexation and aggregate behavior of PMCD.



Scheme 1. Schematic representation of the structures of complexes 1–4.

Result and Discussion

Crystal Structures

Crystals **3** and **4** were synthesized as the complexes of PM- β -CD with 4-HAB and 4-AAB in satisfactory yields (see Experimental Section). Their crystal data and the experimental and refinement parameters are shown in Table 2. Complexes **3** and **4** crystallize in the orthorhombic system and the structural solutions were performed in the space group $P2_12_12_1$. The asymmetric units contain the following: one PM- β -CD, one 4-HAB, and six water molecules for **3**; one PM- β -CD, one 4-AAB, and one water molecule for **4**.

Figure 1 show the host–guest structures of complexes **3** and **4**, in which PM- β -CD assumes a distorted elliptical macrocyclic ring, differing from β -CD in **1** and **2** that maintains the round shape with an approximate sevenfold axis. Every glucose residue of β -CD has a 4C_1 chair conformation, and seven glycosidic oxygen atoms are coplanar within

0.0159 Å (or 0.0136 Å). However, in PM- β -CD, seven glycosidic oxygen atoms comprise a coplane with a mean deviation of 0.4014 Å (or 0.2835 Å). This indicates that the framework of PM- β -CD is more flexible than that of β -CD, as the methylation of all hydroxy groups destroys the intrinsic hydrogen-bonding network of β -CD. The binding structures of the β -CD and PM- β -CD complexes are therefore distinct from each other. In complexes **1** and **2**, the 4-HAB and 4-AAB guests penetrate through the cavity of β -CD and the hydrophobic azo group^[15] is located in the center of the cavity, whereas in complexes **3** and **4**, one of the aromatic rings of the guests enters into the middle area of the PM- β -CD cavity and the azo group is located at the narrow torus rim. This result should be attributed to the diverse hydrophobic characteristics owned by β -CD and PM- β -CD. As is well known, β -CD has a truncated cone structure with a hydrophilic exterior and a hydrophobic inner cavity, whereas the most hydrophobic region is no longer located at the central cavity but at the narrow/broad torus rims made up by the 2-OMe, 3-OMe, and 6-OMe groups once all of the hydroxy groups are methylated.^[10a] In addition, the elliptical cavity of PM- β -CD should prefer to accommodate the planar guests such as aromatic rings. It is also noteworthy that there is an obvious difference in the binding geometries of PM- β -CD complexes **3** and **4**. In complex **3**, the phenol group of 4-HAB is embedded in the PM- β -CD cavity, forming three C–H \cdots π interactions (C5d–H \cdots centroid of aromatic ring 3.530 Å, 133.4°; C6a–H \cdots centroid of aromatic ring 3.744 Å, 121.3°; C2g–H \cdots centroid of aromatic ring 3.756 Å, 162.5°), and the alternative benzene group of 4-HAB is exposed out of the narrow part of the PM- β -CD cavity with two C–H \cdots π interactions (C9e–H \cdots centroid of aromatic ring 3.670 Å, 143.2°; C6e–H \cdots centroid of aromatic ring 3.556 Å, 141.5° where a–g are defined for the labels of seven glucose units of the PM- β -CD cavity). In complex **4**, the benzene group of 4-AAB is embedded in the PM- β -CD cavity with two C–H \cdots π interactions (C5c–H \cdots centroid of aromatic ring 3.860 Å, 145.3°; C5e–H \cdots centroid of aromatic ring 3.268 Å, 128.0°), whereas the aniline group of 4-AAB is located outside the narrow part of the PM- β -CD cavity, forming a C–H \cdots π interaction (C9f–H \cdots centroid of aromatic ring 2.889 Å, 142.1°). Obviously, β -CD provides a similar binding geome-

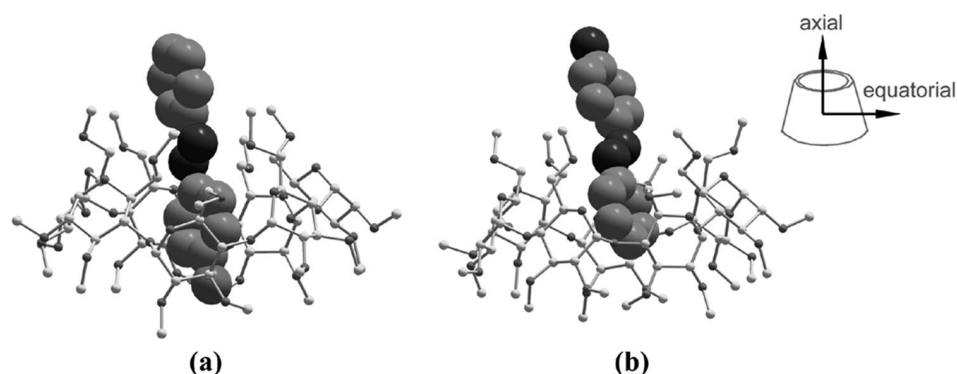


Figure 1. The inclusion structures of complexes **3** (a) and **4** (b).

try with the azobenzene guests, whereas PM- β -CD displays certain regioselectivity upon complexation with 4-HAB and 4-AAB. One possible explanation for the regioselectivity is the different electronegativities of the hydroxy and amino groups, which can be illuminated from the thermodynamic results mentioned below. Moreover, it is noticeable that 4-AAB is included into the host cavity at a more shallow depth than that of 4-HAB, and two N-H \cdots O hydrogen bonds (N1 \cdots O1f 2.439 Å, N1 \cdots O1d 2.503 Å) imply that the amidogen of 4-AAB is inclined to be included into the adjacent PM- β -CD cavity. This binding geometry of complex **4** is favorable to form channel-type aggregation of PM- β -CD complexes, which will be discussed below with the packing structures.

In contrast, it is well known that there are several water molecules in the inner cavities of CDs.^[7a] For example, 6.5 included water molecules were found in the cavity of β -CD dodecahydrate.^[16] However, in complexes **1** and **2**, the water molecules are all located outside the β -CD cavities, which indicates that the inclusion of the azobenzene guests expels the original high-energy water molecules from the inner cavities. Otherwise, no water molecule is located in the PM- β -CD cavity even without any inclusion of guests, according to the previous reports of PM- β -CD crystals.^[9,10b] There is also no water molecule inside the PM- β -CD cavity in complexes **3** and **4**, which demonstrates that the release of high-energy water molecules does not occur during the inclusion process of PM- β -CD with the azobenzene guests. Therefore, we can primarily judge that the driving forces and thermodynamics of the inclusion with guests should be different between β -CD and PM- β -CD.

In the further extended structures, complexes **1** and **2** both present a channel-type arrangement of β -CD in a head-to-head manner, in which the intermolecular multiple hydrogen bonds between the hydroxy groups of two adja-

cent β -CD units emerge to be the dominating factor. On the contrary, PM- β -CD aggregates with in a head-to-tail manner in complexes **3** and **4**, which is in accordance with the reported results of most PM- β -CD complexes.^[7a,14] This pronounced difference between β -CD and PM- β -CD should be attributed to the remarkable reduction of hydrogen bonds among adjacent PM- β -CD torus rims.

Figure 2 shows the extended structures of complex **3** viewed from different orientations. Running along the axial direction of the PM- β -CD cavity, one weak noncovalent C-H \cdots O hydrogen bond (C3 of HAB \cdots O4f 2.514 Å) makes the host-guest complex units arrange in a 1D linear array (Figure 2a). Otherwise, the orientation of two adjacent PM- β -CD units is different, and thus the linear array is with the zigzag shape. In contrast, although the hydroxy groups of two torus rims of the CD cavity are all methylated, which inhibits the formation of axial hydrogen bonds among adjacent PM- β -CDs; PM- β -CDs form multiple C-H \cdots O hydrogen bonds (C3b \cdots O5e 2.358 Å, C6b \cdots O3e 2.559 Å, C9c \cdots O5f 2.487 Å, C3e \cdots O2b 2.557 Å, C4e \cdots O5c 2.479 Å, C3d \cdots O5g 2.560 Å), which makes the exterior walls of PM- β -CDs connected to form a regular plane along the equatorial direction of the cavity (Figure 2b). Therefore, in the overall view of complex **3** (Figure 2c), we prefer the layer-type packing structure.

Although both amino and hydroxy groups are able to form hydrogen bonds, no O-H \cdots O hydrogen bond is observed between the hydroxy group of HAB and the oxygen atoms of PM- β -CD in complex **3**. Instead, there is one O-H \cdots O hydrogen bond (O1 of HAB \cdots O2 of water 2.773 Å) between the hydroxy group of HAB and a water molecule. Much differently, the amino group of 4-AAB in complex **4** is further included into the adjacent PM- β -CD cavity, form-

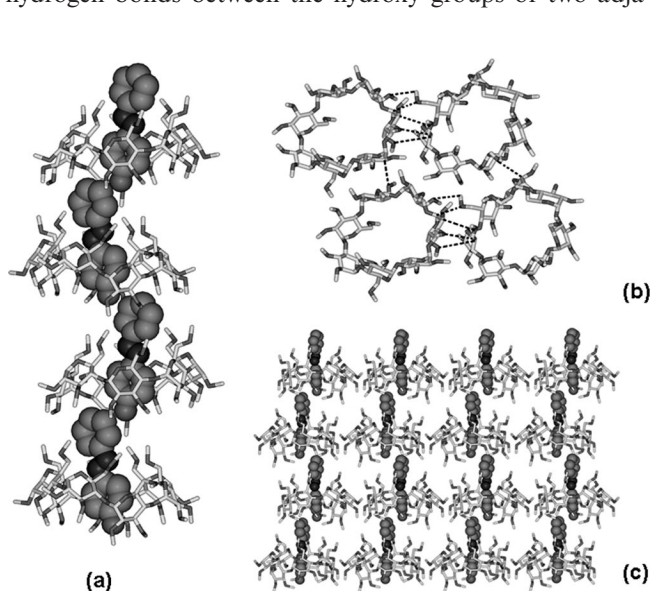


Figure 2. (a) View of the arrangement along the axial direction of the PM- β -CD cavity in complex **3**; (b) view showing the hydrogen-bonding network among the exterior walls of PM- β -CDs in complex **3**; (c) view of the overall packing structure of complex **3**.

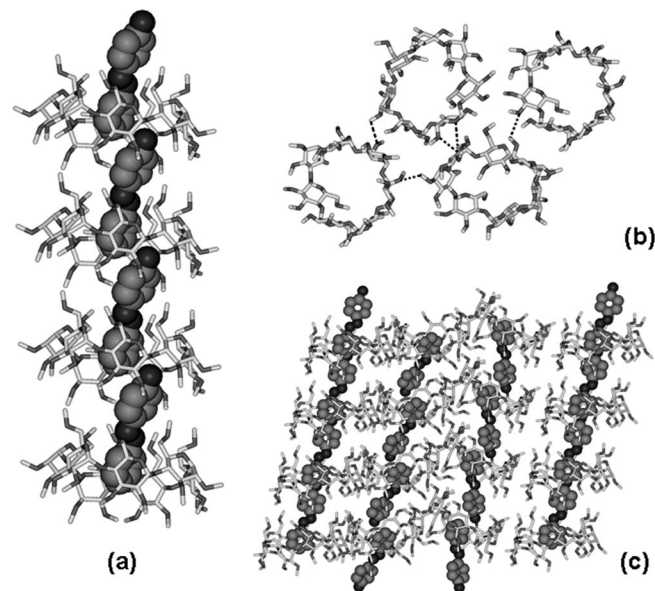


Figure 3. (a) View of the arrangement along the axial direction of the PM- β -CD cavity in complex **4**; (b) view showing the hydrogen-bonding network among the exterior walls of PM- β -CDs in complex **4**; (c) view of the overall packing structure of complex **4**.

ing two strong N–H...O hydrogen bonds. As a result, a typical channel arrangement along the axial direction of the CD cavity is presented in complex **4** (Figure 3a). Moreover, a C–H...O hydrogen bond (C9g...O3a 2.425 Å) also participates in the axial aggregation. In comparison to the channels fabricated in β -CD complexes **1** and **2**, the channel in complex **4** exhibits poorer compactness with a distance between the unrepeatable units of 10.7 Å. It is easily acceptable that methylation of the hydroxy groups elongates the depth of the CD cavity and simultaneously leads to the lack of hydrogen bonds between torus rims of the CD cavities. In the equatorial direction of the PM- β -CD cavity, some C–H...O hydrogen bonds (C8a...O5e 2.322 Å, C3b...O3e 2.564 Å, C4f...O5c 2.594 Å, C7g...O5d 2.584 Å, C9g...O3g 2.455 Å) also connect the exterior walls of the PM- β -CD cavities (Figure 3b). However, unlike the case of complex **3**, complex **4** does not display the regular layer arrangement, but the interlaced channel-type array in the overall view (Figure 3c).

Binding Modes in Solution

Circular dichroism and 2D NMR spectra of complexes **3** and **4** were performed to comprehensively investigate the structure feature and assembly process of PM- β -CD com-

plexes in aqueous solution, which represents two effective means used to analyze the solution structures of CD derivatives and complexes.^[17–19] As can be seen from Figure 4, the achiral guests (4-HAB and 4-AAB) gave two induced circular dichroism (ICD) signals around their corresponding transition band upon inclusion into the chiral microenvironment of the PM- β -CD cavity. In a previous report, neither 4-HAB nor 4-AAB displayed any appreciable circular dichroism signals in the wavelength range from 200–

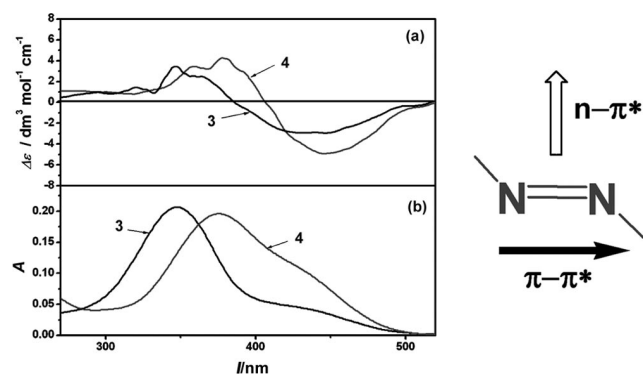


Figure 4. Circular dichroism spectra (a) and UV/Vis absorption spectra (b) of complexes **3** and **4** (a: 2.0×10^{-4} mol dm $^{-3}$ and b: 1.0×10^{-5} mol dm $^{-3}$) in aqueous solution at 25 °C.

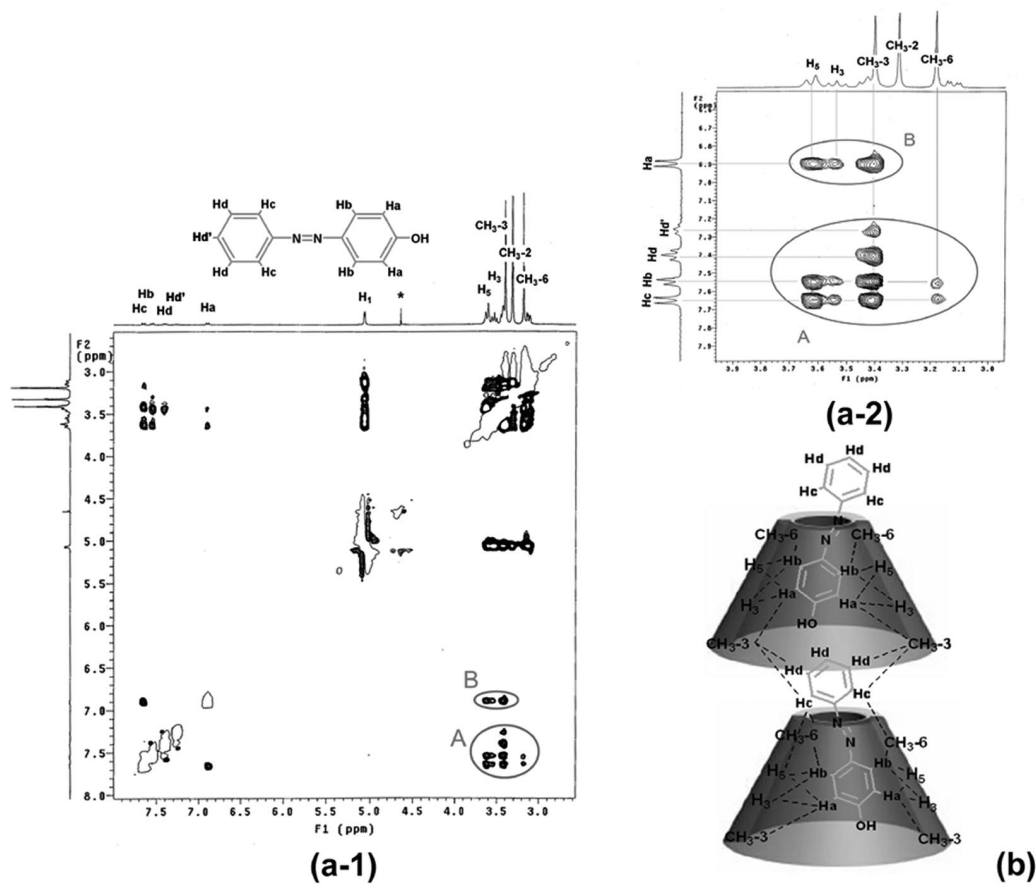


Figure 5. (a) ROESY spectrum of complex **3** (2.6×10^{-3} mol dm $^{-3}$) in D $_2$ O at 25 °C with a mixing time of 250 ms, (b) possible conformation of **3** in D $_2$ O.

500 nm.^[8d] Both **3** and **4** show one positive Cotton effect peak as well as one negative Cotton effect peak (complex **3**: $\Delta\epsilon = 3.42 \text{ dm}^{-3} \text{ mol}^{-1} \text{ cm}^{-1}$ at 348 nm and $\Delta\epsilon = -2.95 \text{ dm}^{-3} \text{ mol}^{-1} \text{ cm}^{-1}$ at 431 nm; complex **4**: $\Delta\epsilon = 4.15 \text{ dm}^{-3} \text{ mol}^{-1} \text{ cm}^{-1}$ at 376 nm and $\Delta\epsilon = -4.94 \text{ dm}^{-3} \text{ mol}^{-1} \text{ cm}^{-1}$ at 446 nm), which is in accordance with $\pi\text{-}\pi^*$ and $n\text{-}\pi^*$ absorbance bands of the azobenzene group, respectively. Therefore, according to the empirical rules on the ICD phenomena of CD complexes,^[20] these ICD signals can result from two possible inclusion orientations: (1) The N=N group is included into the chiral micro-environment of the central cavity with its $\pi\text{-}\pi^*$ transition band nearly parallel to the axial direction of PM- β -CD. (2) The N=N group is located outside the chiral central cavity and likely to stay in the region of the achiral torus rims with its $\pi\text{-}\pi^*$ transition band perpendicular to the axial direction of PM- β -CD.

Further detailed information about the binding geometries of complexes **3** and **4** comes from 2D ROESY experiments. ROESY cross-peaks are indicative of specific proximity relationships between adjacent protons (the distance between protons is generally in the region of 4–5 Å).^[21] Therefore, once the guest molecule is included into the β -CD cavity, the NOE correlation signals between the protons of the guest and the interior protons of the β -CD cavity (H3 and H5) can be observed. For PM- β -CDs, besides the

inner H3 and H5 protons, the substituent methyl groups (CH₃-2, CH₃-3, and CH₃-6) can also provide valuable information about the complex structures by analyzing the correlations between the protons of the methyl groups and the guests. As shown in the ROESY spectrum of complex **3** (Figure 5), several cross-peak signals between PM- β -CD and 4-HAB protons are observed in peaks A and B, suggesting that the 4-HAB guest is included into the cavity of PM- β -CD. Peak B represents the correlations between the H_a protons and the inner PM- β -CD protons including H5, H3, or H6 CH₃-3 protons. In peak A, multiple correlation signals of the H_b and H_c protons with H5, H3, or H6, CH₃-3 protons of the PM- β -CD cavity as well as a weak correlation with the CH₃-6 protons are observed. Moreover, the H_d protons of the benzene group show correlations only with the CH₃-3 protons of the wide rim of the PM- β -CD cavity. It can be inferred from these cross-peaks that the phenol moiety of 4-HAB is embedded into the central cavity from the narrow side of the PM- β -CD cavity. Although considering the superposition of the H3 and H6, H6' peaks, the correlations between the H_c protons and H3 of PM- β -CD are also possible, which makes it difficult to estimate if the benzene group of 4-HAB is also included into the central cavity. However, the correlation peaks between the aromatic protons H_d of the benzene group and H5 or H3 of the inner PM- β -CD are not found. Thus, the hypothesis of

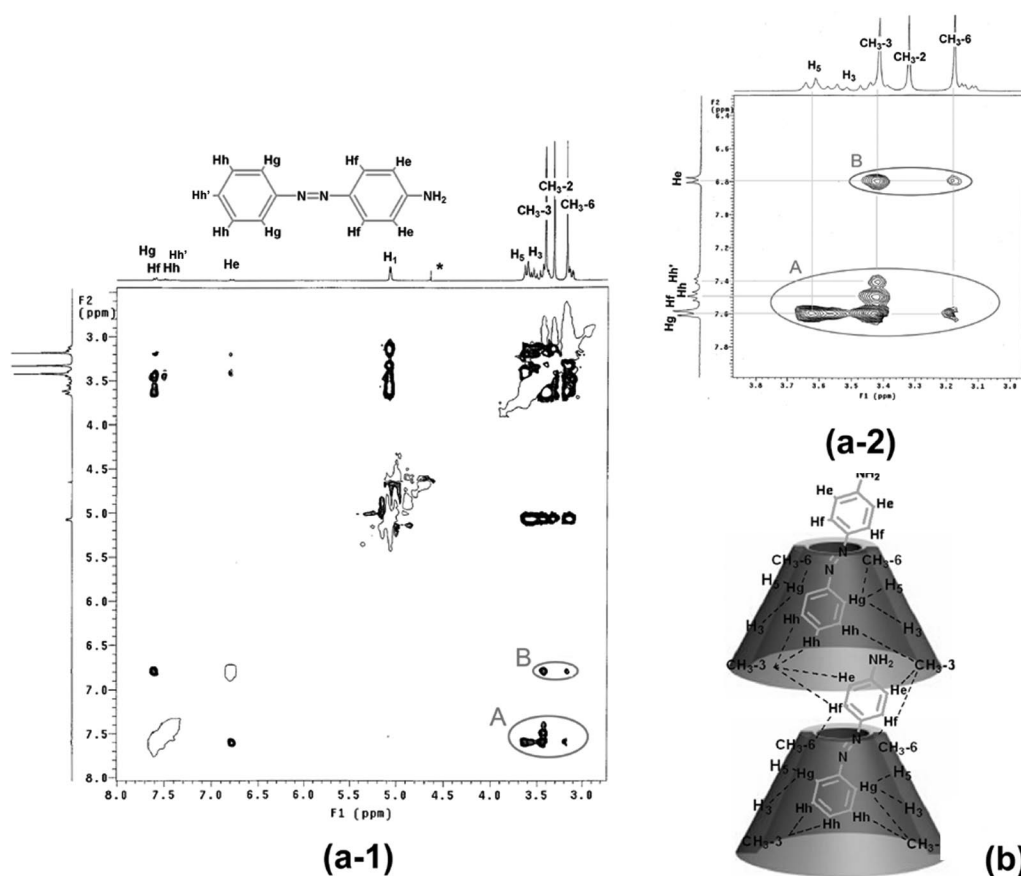


Figure 6. (a) ROESY spectrum of complex about **4** ($3.3 \times 10^{-3} \text{ mol dm}^{-3}$) in D₂O at 25 °C with a mixing time of 250 ms, (b) possible conformation of **4** in D₂O.

the benzene group in the central cavity should be excluded. Furthermore, the only correlation signals of the H_d protons of 4-HAB and the CH_3-3 protons of PM- β -CD illustrate that the 4-HAB guest also has interactions with the wide side of the adjacent PM- β -CD cavity.

As shown in Figure 6, multiple correlation signals are also observed in the 2D ROESY spectrum of complex 4. Peak A exhibits the correlation of the H_g or H_f protons of 4-AAB with H_5 , H_3 , or H_6 , CH_3-3 , and CH_3-6 of PM- β -CD. Moreover, the H_h protons show a correlation signal only with CH_3-3 protons of PM- β -CD. Peak B represents correlations between the H_c protons of 4-AAB and CH_3-3 and CH_3-6 of PM- β -CD. From these correlation peaks, it can be deduced that the benzene moiety of the 4-AAB guest is included into the PM- β -CD cavity. However, because of the superposition of the signals of the H_g and H_f protons, it is also possible that the H_f protons are included into the central cavity. However, the H_c protons of the aniline group have no correlation with any protons of the central cavity of PM- β -CD, excluding the hypothesis of the aniline group in the central cavity. Furthermore, the H_c protons of the aniline group show correlations with the CH_3-3 and CH_3-6 protons of PM- β -CD, suggesting that the aniline moiety of 4-AAB is exposed between the torus rims of two adjacent PM- β -CD cavities. By taking the results of the ICD experiments into account, it can be deduced that the azo groups of 4-HAB and 4-AAB prefer to be located at the narrow torus rim of the PM- β -CD cavity with their $\pi-\pi^*$ transition bands perpendicular to the axial direction of PM- β -CD, and the phenol moiety of 4-HAB and benzene moiety of 4-AAB are included into the central CD cavity.

Complexation Thermodynamics

To provide quantitative and further thermodynamic insight into the inclusion complexation behaviors of 4-HAB or 4-AAB with different CD hosts, the ITC experiments were performed at atmospheric pressure in phosphate aqueous buffer solution (pH 7.2) in the presence of ethanol (20 vol.-%) at 25 °C by using a titration microcalorimeter. The added ethanol is used to solve the poor water solubility of guests. Typical titration curves are shown in Figure 7. According to the ROESY experimental results above, complexes 3 and 4 show $n:n$ binding stoichiometry in aqueous solution with high concentrations up to 2.6 and 3.3 mM. However, the ITC experiment was performed in an water/ethanol solution, where the concentrations of 4-HAB or 4-AAB guests were in the region of about 1.0 mM. The presence of ethanol and the decrease in concentration exert an appreciable negative influence over the aggregation of the obtained complexes. Therefore, under the ITC conditions, PM- β -CD may just form 1:1 simple inclusion complexes with 4-HAB and 4-AAB, but not the $n:n$ aggregates. Actually, we also found that the present host-guest complexation could be well fitted by using the one set of binding sites model in the ITC experiments with the 1:1 model, which implied that the stoichiometry of these two complexes should be 1:1.^[22] The obtained data of complex sta-

bility constants (K_S) and thermodynamic parameters (ΔH° and ΔS°) are listed in Table 1. In a previous report,^[8d] UV spectral titrations were performed in aqueous buffer solution, giving K_S values of 840 M^{-1} for 4-HAB and 2130 M^{-1} for 4-AAB with β -CD, respectively. It is acceptable that the present K_S values of β -CD with azobenzene guests decrease to 339 M^{-1} for 4-HAB and 461 M^{-1} for 4-AAB owing to the addition of ethanol in solution.^[12a,23]

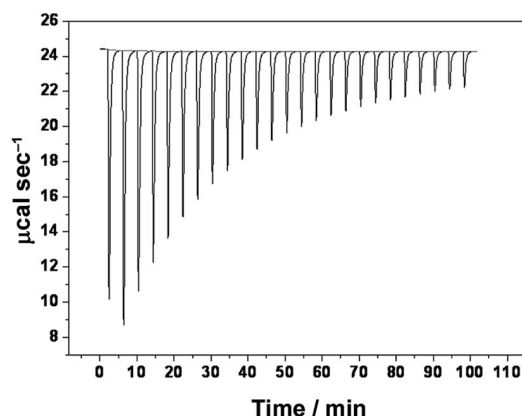


Figure 7. Raw data of the calorimetric titrations of PM- β -CD with 4-AAB in 0.1 M phosphate aqueous buffer solution (pH 7.2) in the presence of ethanol (20 vol.-%) at 25 °C. For sequential 10 μ L injections of CD solution (20.0 mM) into 4-AAB solution (0.93 mM).

Table 1. Complex stability constants (K_S) and standard enthalpy (ΔH°) and entropy changes ($T\Delta S^\circ$) for the inclusion complexation of β -CD and PM- β -CD with azobenzene derivatives in 0.1 M phosphate aqueous buffer solution (pH 7.2) in the presence of ethanol (20 vol.-%) at 25 °C.

Hosts	Guests	K_S / M^{-1}	$-\Delta H^\circ / kJ mol^{-1}$	$T\Delta S^\circ / kJ mol^{-1}$
β -CD	4-HAB	840 ^[a]	–	–
	4-AAB	2130 ^[a]	–24.2 \pm 0.2	–9.8
PM- β -CD	4-HAB	339 \pm 6	–20.4 \pm 0.1	–5.1
	4-AAB	461 \pm 5	–18.2 \pm 0.5	0.6
			–20.8 \pm 0.4	–2.5

[a] Determined by UV/Vis spectral titrations in a phosphate aqueous buffer solution (pH 7.2).^[8d]

The binding processes of β -CD and PM- β -CD with azobenzene guests are all driven by favorable enthalpy changes ($-\Delta H^\circ < 0$), which should be attributed to the significant contribution of hydrophobicity, hydrogen bonds, and van der Waals interactions, as well as C–H \cdots π interactions between host and guest molecules.^[24] Especially, β -CD shows comparative or even more favorable enthalpy changes upon complexation with azobenzene guests than PM- β -CD, although the K_S values of β -CD are 3–5 times lower than those of PM- β -CD. This could result from the pronounced release of high-energy water molecules from the β -CD cavity during the hydrophobic process, which contributes to the favorable enthalpy changes during the course of the complexation of β -CDs; the same does not occur for PM- β -CDs. In contrast, the entropy changes of PM- β -CD with azobenzene guests are much more favorable

than those of β -CD, which could be attributed to two reasons: (1) PM- β -CD possesses a more flexible framework than β -CD; thus, its loss of conformational degrees of freedom upon complexation with guests is certainly less than β -CD. (2) The extended hydrophobic cavity of PM- β -CD can lead to more desolvation effects of the guests. As a result, although the host-guest complexation is enthalpy driven, the large enthalpy changes do not always mean high complex stability, and the molecular selectivity is mainly governed by the entropy term. Moreover, it is notable that only the PM- β -CD complex with the hydroxy derivative guest exhibits a favorable ΔS value of 0.6 kJ mol^{-1} , suggesting that more electrostatic interactions exist between PM- β -CD and the hydroxy group owned by the 4-HAB guest. However, by switching the substituent from a hydroxy group to an amino group, the entropy becomes less favorable, which indicates that there are fewer electrostatic effects in this host-guest system. This result also probably reflects the regioselective complexation of two PM- β -CD complexes, suggesting that the hydroxy group is caged into the cavity, resulting in positive entropy gain as a result of electrostatic interactions, whereas the amino group is outside the cavity and does not contribute to the positive electrostatic gain (Figure 8).

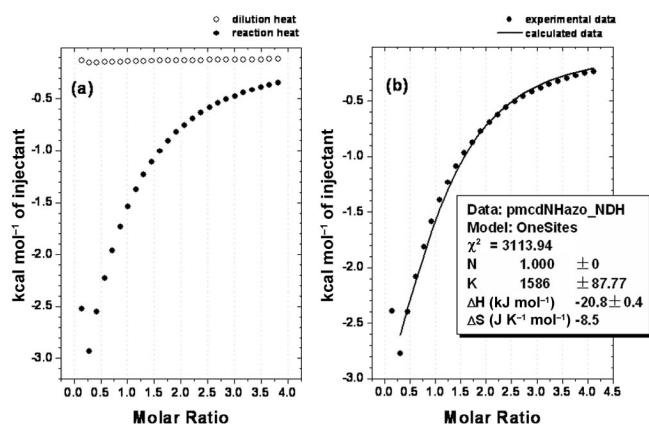


Figure 8. (a) Heat effects of dilution and of complexation of PM- β -CD with 4-AAB for each injection during titration of microcalorimetric experiment; (b) “net” heat effect obtained by subtracting the heat of dilution from the heat of reaction, which was analyzed by computer simulation with the use of the “one set of binding sites” model.

Conclusions

We obtained two complexes, **3** and **4**, of PM- β -CD with azobenzene guests, and their structures were identified by X-ray crystallography, circular dichroism, and 2D NMR spectroscopy and also compared with previous complexes **1** and **2** of β -CD. β -CD includes 4-HAB and 4-AAB guests in the same mode with the azo groups accommodated in the center of the hydrophobic cavity, and further, complexes **1** and **2** present a 1D channel-type arrangement in a head-to-head manner. Conversely, PM- β -CD includes the azobenzene guests regioselectively; the phenol group of 4-HAB

and the benzene group of 4-AAB are immersed into the central cavity of PM- β -CD, and the azo groups are located at the narrow torus rim. Viewed along the axis of the CD cavity, PM- β -CDs are arranged in a contrary head-to-tail manner. The aggregation structures of complexes **3** and **4** are also different from each other, which originate from the considerable complexation regioselectivity of PM- β -CD with two azo guests: layer-type packing structure in complex **3** and channel-type aggregation in complex **4**. Moreover, further ITC investigations indicate that PM- β -CD can form more stable complexes with two azobenzene guests than β -CD, which mainly originates from the more favorable entropy changes during the course of complexation of PM- β -CD with azobenzene guests. The present results will serve us to further understand the inclusion and aggregation behaviors of PM- β -CD and the intrinsic differences between the β -CD and PM- β -CD cavities, which is beneficial in the design and construction of diverse supramolecular assemblies based on CDs.

Experimental Section

Materials: Both 4-hydroxyazobenzene (4-HAB) and 4-aminoazobenzene (4-AAB) were commercially available and used without further purification. Permethylated β -cyclodextrin (PM- β -CD) was synthesized according to a previous literature report.^[25] All other chemicals used in the reactions were reagent grade and used without further purification. Disodium hydrogen phosphate dodecahydrate and sodium dihydrogen phosphate were dissolved in deionized water to make a 0.1 M phosphate aqueous buffer solution of pH 7.2, which was measured by pH electrode for calorimetric titration.

Instruments: Circular dichroism and UV/Vis spectra were recorded with a JASCO J-715S spectropolarimeter and a Shimadzu UV3600 spectrophotometer in a conventional quartz cell (light path 10 mm) in aqueous solution at 25 °C. ^1H and 2D ROESY NMR spectra were obtained in D_2O with a Varian Mercury VX300 instrument with a mixing time of 250 ms. Elemental analysis was performed with a Perkin-Elmer 2400C instrument. The X-ray intensity data for **3** and **4** were collected with a Rigaku MM-007 rotating anode diffractometer equipped with a Saturn CCD Area Detector System by using monochromated $\text{Mo-K}\alpha$ radiation at $T = 113(2) \text{ K}$. Data collection and reduction were performed with the use of the Crystalclear^[26] program. The structures were solved by using direct methods and refined by employing full-matrix least-squares on F^2 (CrystalStructure, SHELXTL-97).^[27] Table 2 summarizes the crystal data and experimental and refinement parameters of **3** and **4**.

CCDC-691287 (for **3**) and -691288 (for **4**) contain the supplementary crystallographic data for this paper. These data can be obtained free of charge from The Cambridge Crystallographic Data Centre via www.ccdc.cam.ac.uk/data_request/cif.

The complex stability constants (K_S) of β -CD and PM- β -CD with 4-HAB and 4-AAB were determined by the method of isothermal titration calorimetry (ITC). The ITC experiments were performed with a Microcal VP-ITC titration microcalorimeter at atmospheric pressure in 0.1 M phosphate aqueous buffer solution (pH 7.2) in the presence of ethanol (20 vol.-%) at 25 °C by using a titration microcalorimeter. The ITC instrument was calibrated chemically by measurement of the complexation reaction of β -CD with cyclohexanol, and the obtained thermodynamic data were shown to be

Table 2. Crystal data and experimental and refinement parameters of complexes **3** and **4**.

	Complex 3	Complex 4
Molecular formula	C ₇₅ H ₁₃₄ N ₂ O ₄₂	C ₇₅ H ₁₃₄ N ₃ O ₃₆
<i>M_r</i> / g mol ⁻¹	1735.84	1644.78
Crystal system	orthorhombic	orthorhombic
Space group	<i>P</i> 2 ₁ 2 ₁ 2 ₁	<i>P</i> 2 ₁ 2 ₁ 2 ₁
<i>Z</i>	4	4
<i>a</i> / Å	14.8450(8)	10.6993(4)
<i>b</i> / Å	22.1705(12)	27.3627(12)
<i>c</i> / Å	27.5443(17)	29.1666(13)
<i>a</i> / °	90	90
<i>β</i> / °	90	90
<i>γ</i> / °	90	90
<i>V</i> / Å ³	9065.4(9)	8538.9(6)
<i>ρ</i> _{calcd.} / g cm ⁻³	1.272	1.279
<i>F</i> (000)	3736	3536
<i>T</i> / K	293(2)	113(2)
<i>μ</i> (Mo- <i>K_α</i>) / mm ⁻¹	0.104	0.102
Crystal size / mm ³	0.16 × 0.14 × 0.14	0.26 × 0.20 × 0.18
<i>θ</i> Range / °	1.48–25.01	1.58–25.00
No. of reflections collected	68276	64982
No. of unique reflections	15829	15017
<i>R</i> _{int}	0.1139	0.0598
GOF	1.181	1.078
Final <i>R</i> indices	0.0983	0.0822
[<i>I</i> > 2σ(<i>I</i>)]	0.1984	0.2175
<i>R</i> ₁ = <i>R</i> indices	0.1126	0.0931
(all data)	0.2059	0.2267

in good agreement (error < 2%) with the literature data. Each solution was degassed and thermostatted by a ThermoVac accessory before titration experiment. Twenty-five successive injections were made for each titration experiment. A constant volume (10 μL/injection) of host solution (20.04–20.32 mM) in a 0.250 mL syringe was injected into the reaction cell (1.4227 mL) charged with guest molecules solution (0.85–1.00 mM) in the same buffer solution. A representative titration curve is shown in Figure 7. Each titration of PM-β-CD into the sample cell gave an apparent reaction heat, caused by the formation of the inclusion complex between the host and guest. The reaction heat decreases after each injection of host molecules because less and less guest molecules are available to form inclusion complexes. A control experiment was carried out in each run to determine the dilution heat by injecting host solution into the same buffer solution containing no guest molecules. The dilution heat determined in these control experiments was subtracted from the apparent reaction heat measured in the titration experiments to give the net reaction heat.

The net reaction heat in each run was analyzed by using “one set of binding sites” model (ORIGIN software) to simultaneously compute the binding stoichiometry (*N*), complex stability constant (*K_S*), standard molar reaction enthalpy (*ΔH°*), and standard deviation from the titration curve. Generally, the first point of titration curve was removed considering that the concentration of host in the cell far exceeded the concentration of the guest. Knowledge of the complex stability constant (*K_S*) and molar reaction enthalpy (*ΔH°*) enabled calculation of the standard free energy (*ΔG°*) and entropy changes (*ΔS°*), according to

$$\Delta G^\circ = -RT \ln K_S = \Delta H^\circ - T\Delta S^\circ$$

where *R* is the gas constant and *T* is the absolute temperature.

A typical curve fitting result for the complexation of PM-β-CD with 4-AAB at pH 7.2 is shown in Figure 8b. To check the accuracy of the observed thermodynamic parameters, two independent ti-

tration experiments were carried out to afford self-consistent thermodynamic parameters.

Complex 3: An ethanol solution of 4-HAB (19.8 mg, 0.1 mmol, 5 mL) was added dropwise to an aqueous solution of PM-β-CD (142.8 mg, 0.1 mmol, 15 mL). The mixture was stirred at 50 °C for 12 h. After removing the insoluble substances by filtration, the resultant solution was kept at 50 °C for several days, and orange complex **3** was collected along with its mother liquor for X-ray crystallographic analysis. Yield: 107.6 mg, 62%. UV/Vis (H₂O): λ (ε, m⁻¹ cm⁻¹) = 348 (2.07 × 10⁴) nm. ¹H NMR (300 MHz, D₂O): δ = 7.65 (d, 2 H, Ar-H), 7.54 (d, 2 H, Ar-H), 7.44–7.24 (m, 3 H, Ar-H), 6.90 (d, 2 H, Ar-H), 5.05 (s, 7H 1-H), 3.72–3.08 (m, 105 H), 3.40 (21 H, 3-OMe), 3.31 (21 H, 2-OMe), 3.18 (18 H, 6-OMe) ppm. C₇₅H₁₂₂O₃₆N₂·6H₂O (1735.87): calcd. C 51.89, H 7.78, N1.61; found C 51.42, H 7.64, N 1.52.

Complex 4: Prepared from 4-AAB and PM-β-CD according to a procedure similar to that described above. Yield: 111.8 mg, 68%. UV/Vis (H₂O): λ (ε, m⁻¹ cm⁻¹) = 379 (1.95 × 10⁴) nm. ¹H NMR (300 MHz, D₂O): δ = 7.64–7.56 (d, 4 H, Ar-H), 7.53–7.37 (m, 3 H, Ar-H), 6.79 (d, 2 H, Ar-H), 5.05 (s, 7H 1-H), 3.72–3.08 (m, 105 H), 3.40 (21 H, 3-OMe), 3.31 (21 H, 2-OMe), 3.18 (18 H, 6-OMe) ppm. C₇₅H₁₂₃O₃₅N₃·H₂O (1644.81): calcd. C 54.77, H 7.66, N 2.55; found C 54.74, H 7.60, N 2.58.

Acknowledgments

This work was supported by the 973 Program (2006CB932900), the National Natural Science Foundation of China (20572052, 20673061, and 20703025), and Special Fund for Doctoral Program from the Ministry of Education of China (20050055004), which are gratefully acknowledged.

- [1] a) S. A. Neposodiev, J. F. Stoddart, *Chem. Rev.* **1998**, *98*, 1959–1976; b) F. M. Raymo, J. F. Stoddart, *Chem. Rev.* **1999**, *99*, 1643–1644.
- [2] a) A. Harada, *Acc. Chem. Res.* **2001**, *34*, 456–464; b) M. Okada, A. Harada, *Org. Lett.* **2004**, *6*, 361–364.
- [3] a) P. N. Taylor, M. J. O’Connell, L. A. McNeill, M. J. Hall, R. T. Aplin, H. L. Anderson, *Angew. Chem.* **2000**, *112*, 3598–3602; *Angew. Chem. Int. Ed.* **2000**, *39*, 3456–3460; b) F. Cacialli, J. S. Wilson, J. Michels, C. Daniel, C. Silva, R. H. Friend, N. Severin, P. Samori, J. P. Rabe, M. J. O’Connell, P. N. Taylor, H. L. Anderson, *Nat. Mater.* **2002**, *1*, 160–164.
- [4] a) H. Murakami, A. Kawabuchi, K. Kotoo, M. Kunitake, N. Nakashima, *J. Am. Chem. Soc.* **1997**, *119*, 7605–7606; b) Y. Kawaguchi, A. Harada, *Org. Lett.* **2000**, *2*, 1353–1356; c) Q.-C. Wang, D.-H. Qu, J. Ren, K. Chen, H. Tian, *Angew. Chem.* **2004**, *116*, 2715–2719; *Angew. Chem. Int. Ed.* **2004**, *43*, 2661–2665; d) D.-H. Qu, Q.-C. Wang, J. Ren, H. Tian, *Org. Lett.* **2004**, *6*, 2085–2088.
- [5] a) A. Harada, J. Li, M. Kamachi, *Nature* **1993**, *364*, 516–518; b) E. Ikeda, Y. Okumura, T. Shimomura, K. Ito, T. Hayakawa, *J. Chem. Phys.* **2000**, *112*, 4321–4325; c) M. Saito, T. Shimomura, Y. Okumura, K. Ito, R. Hayakawa, *J. Chem. Phys.* **2001**, *114*, 1–3.
- [6] J. Szejtli, T. Osa in *Comprehensive Supramolecular Chemistry* (Eds.: J. L. Atwood, J. E. Davies, D. D. MacNicol, F. Vögtle), Pergamon/Elsevier, Oxford, **1996**, vol. 3.
- [7] a) K. Harata, *Chem. Rev.* **1998**, *98*, 1803–1827; b) M. Añibarro, K. Gessler, I. Usön, G. M. Sheldrick, K. Harata, K. Uekama, F. Hirayama, Y. Abe, W. Saenger, *J. Am. Chem. Soc.* **2001**, *123*, 9880–9888; c) J. L. Clark, B. R. Booth, J. J. Stezowski, *J. Am. Chem. Soc.* **2001**, *123*, 9889–9895.
- [8] a) Y. Liu, Z. Fan, H.-Y. Zhang, C.-H. Diao, *Org. Lett.* **2003**, *5*, 251–254; b) Y. Liu, Z. Fan, H.-Y. Zhang, Y. W. Yang, F.

- Ding, S.-X. Liu, X. Wu, T. Wada, Y. Inoue, *J. Org. Chem.* **2003**, *68*, 8345–8352; c) Y. Liu, Y.-L. Zhao, H. Y. Zhang, E. C. Yang, X. D. Guan, *J. Org. Chem.* **2004**, *69*, 3383–3390; d) Y. Liu, Y.-L. Zhao, Y. Chen, D.-S. Guo, *Org. Biomol. Chem.* **2005**, *3*, 584–591.
- [9] T. Steiner, W. Saenger, *Angew. Chem.* **1998**, *110*, 3628–3632; *Angew. Chem. Int. Ed.* **1998**, *37*, 3404–3407.
- [10] a) I. Stefan, W. L. D. Frieder, *Starch/Stärke* **1996**, *48*, 225–332; b) R. C. Mino, A. B. Susan, T. M. Welcome, M. D. Pamela, *Chem. Commun.* **2004**, 2216–2217.
- [11] R. I. Gelb, L. M. Schwartz, *J. Inclus. Phenom. Mol. Recognit. Chem.* **1989**, *7*, 537–543.
- [12] a) K. Kano, R. Nishiyabu, T. Asada, Y. Kuroda, *J. Am. Chem. Soc.* **2002**, *124*, 9937–9944; b) K. Kano, H. Kitagishi, S. Tamura, A. Yamada, *J. Am. Chem. Soc.* **2004**, *126*, 15202–15210; c) K. Kano, R. Nishiyabu, R. Doi, *J. Org. Chem.* **2005**, *70*, 3667–3673.
- [13] A. Takashi, K. Yudai, T. Shinji, T. Minoru, *J. Chromatogr. A* **1999**, *845*, 455–462.
- [14] a) K. Harata, K. Uekama, M. Otagiri, F. Hirayama, *Chem. Lett.* **1983**, 1807–1810; b) K. Harata, F. Hirayama, T. Imai, K. Uekama, M. Otagiri, *Chem. Lett.* **1983**, 1549–1552; c) A. Grandeury, S. Petit, G. Gouhier, V. Agassea, G. Coquerela, *Tetrahedron: Asymmetry* **2003**, *14*, 2143–2152; d) J.-L. Mieusset, D. Krois, M. Pacar, L. Brecker, G. Giester, U. H. Brinker, *Org. Lett.* **2004**, *6*, 1967–1970.
- [15] a) T. Kozlecki, A. Sokolowski, K. A. Wilk, *Langmuir* **1997**, *13*, 6889–6895; b) Y. Sueishi, M. Kasahara, M. Inoue, K. Matsueda, *J. Inclus. Phenom. Mol. Recognit. Chem.* **2003**, *46*, 71–75.
- [16] K. Lindner, W. Saenger, *Carbohydr. Res.* **1982**, *99*, 103–115.
- [17] a) X. Zhang, W. M. Nau, *Angew. Chem.* **2000**, *112*, 555–557; *Angew. Chem. Int. Ed.* **2000**, *39*, 544–547; b) B. Mayer, X. Zhang, W. M. Nau, G. Marconi, *J. Am. Chem. Soc.* **2001**, *123*, 5240–5248.
- [18] a) S.-Y. Yang, M. M. Green, G. Schultz, S. K. Jha, A. H. E. Muller, *J. Am. Chem. Soc.* **1997**, *119*, 12404–12405; b) S. R. McAlpine, M. A. Garcia Garibay, *J. Am. Chem. Soc.* **1998**, *120*, 4269–4275; c) Y. Inoue, T. Wada, N. Sugahara, K. Yamamoto, K. Kimura, L.-H. Tong, X.-M. Gao, Z.-J. Hou, Y. Liu, *J. Org. Chem.* **2000**, *65*, 8041–8050; d) H. Nakashima, Y. Takenaka, M. Higashi, N. Yoshida, *J. Chem. Soc. Perkin Trans. 2* **2001**, 2096–2103; e) Y. Takenaka, M. Higashi, N. Yoshida, *J. Chem. Soc. Perkin Trans. 2* **2002**, 615–620.
- [19] Y. Liu, Y.-L. Zhao, H.-Y. Zhang, Z. Fan, D.-S. Guo, F. Ding, *J. Phys. Chem. B* **2004**, *108*, 8836–8843.
- [20] a) K. Harata, H. Uedaira, *Bull. Chem. Soc. Jpn.* **1975**, *48*, 375–378; b) M. Kajtár, C. Horvath-Toro, E. Kuthi, J. Szejtli, *Acta Chim. Acad. Sci. Hung.* **1982**, *110*, 327–355; c) M. Kodaka, *J. Am. Chem. Soc.* **1993**, *115*, 3702–3705.
- [21] H. J. Schneider, F. Hacket, V. Rüdiger, *Chem. Rev.* **1998**, *98*, 1755–1785.
- [22] a) P. R. Cabrer, E. Alvarez-Parrilla, F. Mejjide, J. A. Seijas, E. R. Núñez, J. V. Tato, *Langmuir* **1999**, *15*, 5489–5495; b) P. R. Cabrer, E. Alvarez-Parrilla, W. Al-Soufi, F. Mejjide, E. R. Núñez, J. V. Tato, *Supramol. Chem.* **2003**, *15*, 33–43.
- [23] T. Yamada, T. Imai, K. Ouchi, M. Otagiri, F. Hirayama, K. Uekama, *Chem. Pharm. Bull.* **2000**, *48*, 1264–1269.
- [24] a) M. Rekharsky, Y. Inoue, *J. Am. Chem. Soc.* **2000**, *122*, 10949–10955; b) M. Rekharsky, Y. Inoue, *J. Am. Chem. Soc.* **2002**, *124*, 813–826.
- [25] J. Boger, R. J. Corcoran, J.-M. Lehn, *Helv. Chim. Acta* **1978**, *61*, 2190–2218.
- [26] *CrystalStructure 3.7.0 and Crystalclear 1.36: Crystal Structure Analysis Package*, Rigaku and Rigaku/MS (2000–2005), The Woodlands, TX.
- [27] G. M. Sheldrick, *SHELX97*, University of Göttingen, Germany, **1997**.

Received: August 29, 2008
Published Online: January 2, 2009